

## Improvement of Silver Nanoparticles Synthesis by *Monascus purpureus* using Gamma Irradiation

Ahmed I. El-Batal<sup>1</sup>, Ashraf F. El-Baz<sup>2</sup>, Farag M. Abomosalam<sup>1</sup>,  
Ahmed A. Tayel<sup>2</sup>

*1*Drug Radiation Research Dep., Biotechnology Division, National Center for Radiation Research and Technology (NCRRT), Atomic Energy Authority, Egypt.

*2* Genetic Engineering and Biotechnology Research Institute - University of Sadat City, Egypt.

---

### Abstract

Aqueous dispersion of highly stable silver nanoparticles were synthesized using gamma irradiation with *Monascus purpureus* supernatant molecules as reducing and stabilizing agent. The formation of Nano sized silver was confirmed by its characteristic surface Plasmon absorption peak around 420nm in UV-VIS spectra. The size of the silver nanoparticles can be turned by controlling the radiation dose and mixing method of AgNO<sub>3</sub> solution with *Monascus purpureus* supernatant (irradiation process). Dynamic light scattering (DLS) measurement and Transmission electron microscope (TEM) of the synthesized nanoparticles indicated that the size depend on dose and irradiation process . The irradiation was carried out at doses from 1 to 25kGy . XRD analysis of the silver confirmed the formation of metallic silver. Fourier transform infra-red (FTIR) spectroscopic data indicate abounding of Ag nanoparticles with *Monascus purpureus* supernatant molecules. The obtained Ag nanoparticle dispersion was stable for over 3 months at room temperature.

**Key words:** Biosynthesis; Ag nanoparticle; DLS; TEM; FTIR

---

### 1-Introduction:

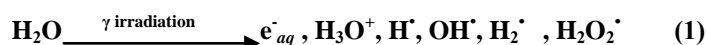
Gamma radiation has been proved to be a simple and efficient method for silver nanoparticles synthesis, the synthesis of nanoparticles through the gamma radiation route requires an aqueous system, room temperature and ambient pressure ( Li *et al .*, 2012). The preparation and study of metal nanoparticles is interest in both research and technology, because of their potential applications in areas such as catalysis, Nano electronics, optical filters, electromagnetic interference shielding and surface Raman scattering (Ramnani *et al .*, 2007). The surface Plasmon absorbance (SPA) properties of nanoparticles have direct relationship with the size, shape, and chemical composition of nanoparticles, intensity and wavelength shift of SPA absorption spectrum were used to follow thgrowth or particle size (Naghavi *et al .*, 2010).

Various methods of synthesizing colloidal silver nanoparticles using metal salts as precursors have been reported, namely chemical reduction, photochemical, electrochemical, microwave processing and irradiation,

---

irradiation induced reduction synthesis which offers some advantages over the conventional methods, because of its simplicity, it provides metal nanoparticles in fully reduced, highly pure and highly stable state (**Ramnani et al.**, 2007).

In this method, the aqueous solution of metal salt is exposed to  $\gamma$ -rays; the species hydrated electron and hydrogen atoms arising from radiolysis of water are strong reducing reagents and they reduce the metal ion to zero valent state (**Marignier et al.**, 1985).



The radiolytic method is particularly suitable for generation of metal NPs in solution, because the radiolytically generated species exhibit strong reducing power and reduction of metal ions occur at each encounter. A blue shift of the silver Plasmon absorption band resulting from the electronic polarization of Ag particles, was observed for aqueous solution in the case of electron transfer from the free radicals generated radiolytically or photolytically due to adsorption of ions or molecules on metal clusters (**Temgire et al.**, 2004).

The radiolytic method is suitable for generation of metal particles, particularly silver, in solution (**Remita et al.**, 2005). The amount of zerovalent nuclei can be controlled by varying the dose of the irradiation (**Eisa et al.**, 2011). Generally, Polymer/metal Nano composites can be obtained by two different approaches, namely, ex situ and in situ techniques. In the ex situ approach, polymerization of monomers and formation of metal nanoparticles were separately performed, and then they were mechanically mixed to form Nano composites. In the in situ methods, metal nanoparticles are generated inside a polymer matrix by decomposition (e.g., thrombolysis, photolysis, radiolysis, etc.) or by chemical reduction of a metallic precursor dissolved in the polymer. A commonly employed in situ method is the dispersion process, in which the solutions of the metal precursor and the protective polymer are combined, and the reduction is subsequently performed in solution (**Eksik et al.**, 2010). In situ nanoparticle generation can be attained by using three approaches:

- 1-Ag<sup>+</sup> reduction in solution, followed by solvent evaporation and film formation (**Khanna et al.**, 2005)
- 2-The silver ions can be absorbed within a preformed polymer film immersed in a Ag<sup>+</sup> solution and then reduced (**Gaddy et al.**, 2004) and
- 3- The NPs are nucleated and grown in the solid state (**Porel et al.**, 2005)

Silver NP nucleation and growth can be easily followed by absorption spectroscopy, since the surface plasmon resonance (SPR) band is sensitive to particle size (**Kelly et al.**, 2003), morphology, dispersity, dielectric properties of the supporting medium and aggregation (**Sun & Xia**, 2003).

The irradiation, as a new method, had been extensively used to prepare Nano-scale clusters and materials; the most studies of irradiation have been focus on the synthesis of metallic clusters and crystals (**Yang et al.**, 2002).

Recently, metal nanoparticles (NPs) have stimulated worldwide investigation because of their remarkable physical and chemical properties relative to their bulk solid counterparts, due to their large proportion of high-energy surface atoms (Murphy, 2002). As a consequence, the production of NPs has attracted an enormous amount of attention in recent years. Silver NPs (Ag-NPs) have a number of superior properties and are widely used in different fields such as in medicine because of their antibacterial properties, in electronics as thick-film conductor conductivities, in surface-enhanced resonance Raman scattering, in optical biosensors, and in oxidative catalysis, photocatalysis, and chemical analysis (Shameli *et al.*, 2010). In addition, nanosized silver colloid ink has recently been used for inkjet printing (Lee *et al.*, 2005). Recently, the investigation of the attractive antibacterial activities of Ag-NPs has reclaimed importance due to an increase of bacterial resistance to antibiotics caused by their overuse. Presently, Ag-NPs displaying antibacterial activity are being synthesized. Antibacterial activity of the silver-containing materials can be used, for example, in medicine to reduce infections as well as to prevent bacterial colonization on prostheses, dental materials, vascular grafts, catheters, human skin, and stainless steel materials (Panacek *et al.*, 2006). The Ag-NPs are normally short lived in aqueous solution as they agglomerate quickly.

Numerous methods have been utilized for the synthesis and stabilization of Ag-NPs. Problems with the stability of the produced colloidal Ag-NPs dispersions have been solved by the addition of polymers and surfactants (Ahmad *et al.*, 2010). Such complications do not occur if the NPs are deposited on a stable inert carrier. Ag-NPs have been deposited on glass (Li *et al.*, 2003).

The use of  $\gamma$ -irradiation in the preparation of Ag-NPs has been demonstrated to have a number of highly advantageous properties compared with conventional chemical and photochemical methods, namely (Shameli *et al.*, 2010)

- The controlled reduction of silver ions can be carried out devoid of using surplus reducing agents or producing any undesired oxidation products from the reductants.
- The method provides Ag-NPs in completely reduced, extremely pure, and very stable states.
- The reducing agent is generated uniformly in the solution.
- The process is uncomplicated and uncontaminated.
- The  $\gamma$ -ray irradiation is harmless.
- No undesirable impurities similar to silver oxide are introduced.

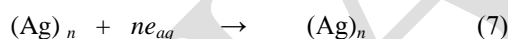
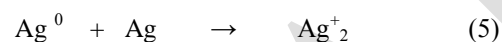
This novel method in comparison to our other works, consist of controlled reduction without any undesired oxidation products, extremely stable colloids, very pure silver ions reduced to NPs in the high  $\gamma$ -irradiation doses. Stabilizer was used as the protective colloid, preventing the Ag-NPs from aggregation. At different  $\gamma$ -irradiation doses, both reduction and fragmentation of large Ag-NPs were found to have occurred simultaneously, and the particle size of the Ag-NPs decreased or increased at different

irradiation doses. Using this method, the researchers were able to obtain Ag-NPs of different sizes by controlling the  $\gamma$ -irradiation dose.

AgNO<sub>3</sub> separated to Ag<sup>+</sup> and NO<sub>3</sub><sup>-</sup> ions in the aqueous solution as shown in Equation 2. The solvated electrons, ie,  $e^-_{aq}$ , and H atoms are strong reducing agents; therefore, in the following step, they easily reduced silver ions down to the zerovalent state (Equations 3 and 4) (Sheikh *et al.*, 2009).



Silver atoms formed by the irradiation tended to coalesce into oligomers (Equation 5), which progressively grew into large clusters (Equation 6). The aqueous electrons reacted with the Ag<sup>+</sup> clusters to form the relatively stabilized Ag clusters (Equation 7) (Janata *et al.*, 1994).



We presented an improved gamma radiation approach for the synthesis of silver nanoparticles. Here we use *Monascus purpureus* supernatant, which has been proved to be biocompatible components, as a template for nanoparticles growing. The results of gamma irradiation investigate that low and high doses effect on the size and optical absorption of Ag-NPs. Reduction of metal is an important defense mechanism in microorganisms as a way to manage metal toxicity. The inherent, clean, nontoxic and environmentally friendly ability of eukaryotic and prokaryotic microorganisms to form the metal nanoparticles is particularly important in the development of Nano biotechnology. New methods have been developed to control disparity, chemical composition, the size, and the shape to get the best particles which can be well applied in different fields of science. However, there is a growing need to understand the basics of this technique to facilitate application of the new methodology to laboratory and industrial needs (Biswal *et al.*, 2011).

*Monascus spp.* produces a complex mixture of three categories of pigments, orange, red, and yellow, each with two components of polyketide origin.

These are secondary metabolites with a common azaphilone skeleton (Zagoldie *et al.*, 2012 and Carvalho *et al.*, 2003). The orange pigment includes monascorubrin and rubropunctatin, possessing the Oxo lactone ring, red pigment includes monascorubramine and rubropunctamine that are the nitrogen analogues of the orange pigment and yellow pigment includes monascin and ankaflavin (Zhou *et al.*, 2009). Among these pigments, the red

pigment is of high demand, especially for its use in meat products to substitute nitrites (Fabre *et al.*, 1993). *Monascus* pigments, which are produced by various species of *Monascus*, have been used as a natural colorant and as traditional natural food additives in East Asia (Carels and Shepherd, 1977). They are synthesized from polyketide chromophores and  $\beta$ -keto acids by esterification (Ju *et al.*, 1996). They are stable in a wide range of pH and heat (Kim *et al.*, 1977). Metabolic products from *Monascus* species in the fermentation are commonly utilized as pigments of food additives or as antimicrobial agents. The components isolated from the fungus exert several biological actions and produce hypocholesterolemic, liver protective and antitumor effects (Endo, 1980). *Monascus purpureus* extracellular pigments has anti-oxidant activity and high reducing power, with this microorganism, fermentative production of pigments can be obtained in both solid-state and submerged cultivation (Carels *et al.*, 1977)

## 2. Material and methods

### 2.1. Microorganism

Fungal culture of *Monascus purpureus* NRRL 1992 was obtained from the National Center for Radiation Research and Technology, Cairo, Egypt. Was maintained on Sabouraud dextrose agar plates at 4°C and sub cultured periodically. Cultures reactivated by transferring onto fresh Sabouraud agar plates and cultured at 30°C for 5–7 days were used for inoculum preparation.

### 2.2. Materials

AgNO<sub>3</sub> (99%), agar, glucose, yeast extract, NEED (N (1-naphthyl) ethylenediaminedihydrochloride) and DPPH from (sigma Aldrich). deionized water prepared in laboratory. All other reagents used as received without any treatment.

### 2.3. Supernatant (Filtrate) preparation

Erlenmeyer flasks (250 mL) containing 50 mL of medium (yeast extract 5gm/l, starch 20gm/l and glucose 15gm/l) at pH (5.5) were inoculated with 250  $\mu$ L (1%, v/v) of a conidial and mycelial suspension. For the preparation of this suspension, 5-7 day-old cultures were scraped from the surface of Sabouraud agar, added to a 0.85% NaCl saline sterile solution, and mixed until a homogeneous solution was obtained. The inoculated flasks were incubated at 27 °C on a rotatory shaker at 100 rpm for 7 days. The cultures were centrifuged at 12,000 rpm for 15 minutes and their supernatants were used for silver nanoparticles synthesis and other assay.

### 2.4. Preparation of silver colloids by $\gamma$ -irradiation:

#### 2.4.1. Gamma irradiation source

The process of irradiation was carried out at the National Center for Radiation Research and Technology (NCRRT). The facility used was <sup>60</sup>Co-Gamma chamber 4000-A-India. Irradiation was performed using <sup>60</sup>Co-gamma rays at a dose rate from 3.33 to 83.25kGy/hr. at the time of the experiment. In this process, <sup>60</sup>Co  $\gamma$ -rays interact with matters in the solution

mainly by photoelectric absorption and Compton scattering to produce free electrons and also hydrated electrons induced from water radiolysis. Together, these electrons reduce the  $\text{Ag}^+$  into  $\text{Ag}^0$ .

#### **2.4.2. Radiation processing (mixing process):**

##### **2.4.2.1. Ex situ irradiation process:**

*Monascus purpureus* supernatant or and  $\text{AgNO}_3$  solution (1mM) were separately irradiated at different doses from 1 to 25kGy using  $^{60}\text{Co}$   $\gamma$ -rays, and then they were mixed to form Nano. The irradiated supernatant was mixed with irradiated and Nan irradiated  $\text{AgNO}_3$  solution (1mM, v/v) and incubated at room temperature in dark.

#### **2.7. Characterization of silver nanoparticles**

##### **2.7.1. UV-VIS spectral analysis:**

Preliminary characterization of the silver nanoparticles was carried out using UV-visible spectroscopy (JASCO-Japan-model V- 560) at a resolution of 1 nm. Noble metals, especially gold (Au) and silver (Ag) nanoparticles exhibit unique and tunable optical properties on account of their surface Plasmon resonance (SPR), dependent on shape, size and size distribution of the nanoparticles (Tripathy *et al.*, 2010). The reduction of silver ions was monitored by measuring the UV-visible spectra of the solutions from 300 to 800 nm. The *Monascus* supernatant was used as blank.

##### **2.7.2. Dynamic light scattering (DLS)**

Average particle size and size distribution were determined by the dynamic light scattering (DLS) (Katrin *et al.*, 2011) technique (PSS-NICOMP 380-ZLS, USA) to both in situ and ex situ irradiated samples. Before measurements, the samples were diluted 10times with deionized water. 250 $\mu\text{l}$  of suspension were transferred to a disposable low volume cuvette. After equilibration to a temperature of 25°C for 2 min, five measurements were performed using 12 runs of 10 s each.

##### **2.7.3. Transmission Electron Microscopy (TEM)**

The particle size and shape were observed by TEM (Shameli *et al.*, 2010) (JEOL electron microscope JEM-100 CX) operating at 80 kV accelerating voltage. The prepared Ag-NPS formed by in situ and ex situ radiation was diluted 10 times with deionized water. A drop of the suspension was dripped into coated copper grid and allowed to dry at room temperature.

##### **2.7.4. Fourier Transform Infrared Spectroscopy (FT-IR)**

A drop of colloidal Ag-NPs formed by in situ and ex situ radiation was mixed with KBr powder and, after drying, compressed to form a disc. The discs were later subjected to FTIR spectroscopy measurement. These measurements were recorded on a JASCO FT-IR -3600 and spectrum was collected at a resolution of 4 $\text{cm}^{-1}$  in wave number region of 400 to 4000 $\text{cm}^{-1}$ . For comparison, *Monascus purpureus* supernatant was measured by the

same process. FT-IR measurements were carried out in order to obtain information about chemical groups present around Ag-NPs for their stabilization and understand the transformation of functional groups due to reduction process.

### 2.7.5. Energy Dispersive X- ray (EDX):

The Energy Dispersive X- ray (EDX-model-OXFORD) spectroscopy was performed on scanning Electron Microscope( SEM- JEOL-JEM-5400) equipped with an EDX detector and EDX spectrum was measured at 10KV accelerating voltage .solid sample was prepared by drying of silver Nanoparticles solution on plastic disc and dried at room temperature.

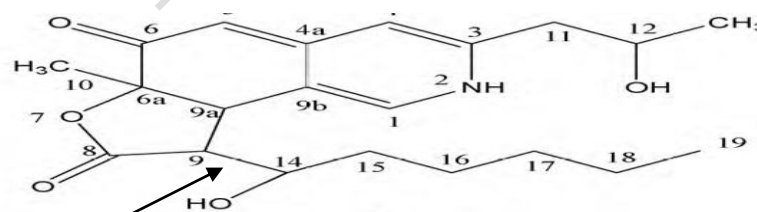
### 2.7.6. X-ray diffraction (XRD) analysis

The reaction mixture embedded with the silver nanoparticles was placed on glass slid to form film and dried at room temperature to use for X-ray diffraction (XRD) analysis. XRD scans were obtained using a Rigaku model D/ max2000PC X-ray diffractometer operating with a Cu anode at 40 Kv and 5 0 mA in the range of  $2\theta$  value between  $20^\circ$  and  $100^\circ$  with a speed of  $2^\circ/\text{min}$ . Prior to peak width measurement, each diffraction peak was corrected for background scattering and was stripped of  $K\alpha_2$  portion of the diffracted intensity. Crystallite size, L, was calculated from Scherrer's equation (Lei & Fan, 2006),  $D = K \lambda / \beta_{1/2} \cos\theta$  for peak broadening from size effects only. Where  $\lambda$  is the wavelength of X-rays used (1.5418Å),  $\beta$  is the full width at half-maximum (fwhm) intensity of the diffraction line,  $\theta$  is the Bragg angle for the measured hkl peak, and K is a constant equal to 0.9 for Ag<sub>0</sub>.

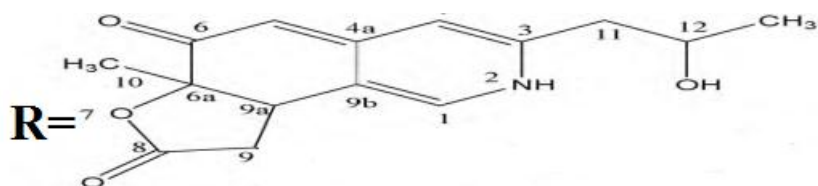
## 3. Results and discussions

### 3.1. Ex situ irradiation process mechanism of reduction

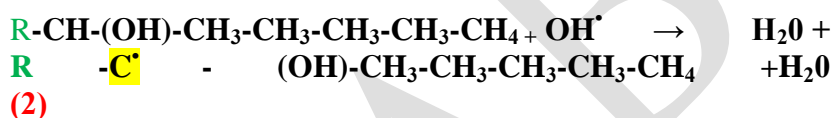
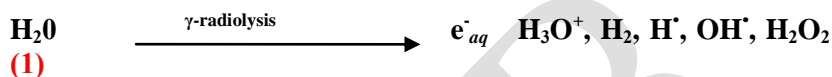
The mechanism of radio lytic reduction of aqueous solution is carried out by organic radicals formed (Rao *et al.*, 2010). *Monascus purpureus* supernatant molecules (especially red pigments) play an important role in scavenging the free radicals and converted into organic radicles.



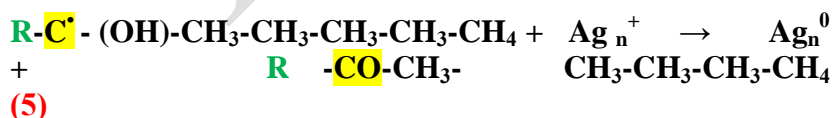
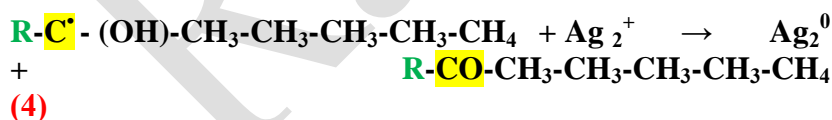
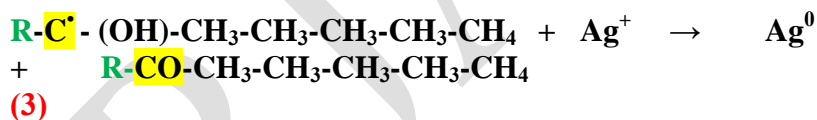
Red pigment structure of *Monascus purpureus* (Mukherjee *et al.*, 2010) as examples.



We suggest the following provisional mechanism for ex situ irradiation process for reduction, which is consistent with similar studies on the irradiation reduction of Ag-NPs in other solutions (Temgire *et al.*, 2004). The growth of silver nanoparticles by reduction of  $\text{Ag}^+$  to  $\text{Ag}^0$  is step wise show in the following Eqs. (1), (2), (3), (4) and (5)



A secondary radical is formed ( $\text{R-C}^\cdot\text{-(OH)-CH}_3\text{-CH}_3\text{-CH}_3\text{-CH}_3\text{-CH}_4$ ) which efficiently reduces the precursor metal ions  $\text{Ag}^+$  to  $\text{Ag}^0$ .



The hydroxyl radicals from the water radiolysis were scavenged efficiently by *Monascus purpureus* supernatant molecules (resonance system  $\text{R-CH-(OH)-CH}_3\text{-CH}_3\text{-CH}_3\text{-CH}_3\text{-CH}_4$ ) to yield a secondary radical ( $\text{R-C}^\cdot\text{-(OH)-CH}_3\text{-CH}_3\text{-CH}_3\text{-CH}_3\text{-CH}_4$ ), that reduce  $\text{Ag}^+$  to  $\text{Ag}^0$ , this is consistent with similar studies on the irradiation reduction of Ag-NPs in other solutions (Mostafavi *et al.*, 2002).

Since the electrochemical potential of the organic radical is more positive than that of the  $\text{Ag}^+/\text{Ag}^0$  system so reaction of secondary radicals formed with



Ag<sup>+</sup> ions is relatively slow (Henglein, 1998). After mixing of irradiated *Monascus purpureus* supernatant with AgNO<sub>3</sub> solution (1mM), the dispersion became yellowish brown and deep red depend on dose of radiation as in fig (1), yellowish brown color indicating the formation of highly stable and uniform-sized silver nanoparticles (Liu *et al.* , 2009).

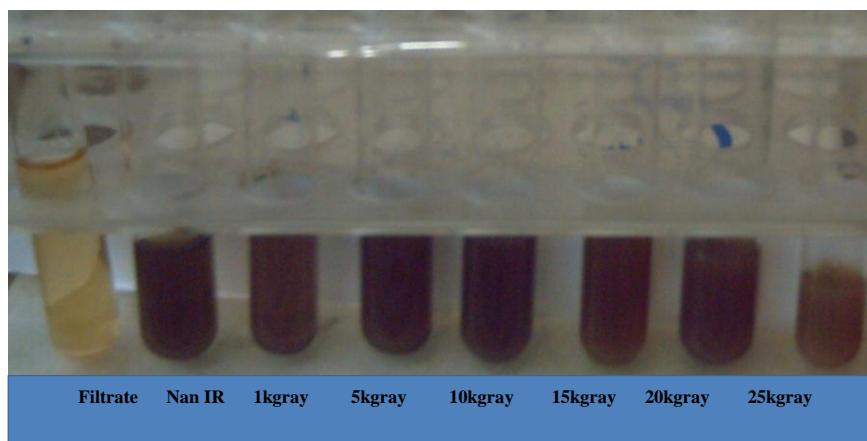


**Fig (1): Image of Ag-NPs prepared by ex situ irradiation process under different doses of irradiation ranged from 1kGy to 25kGy.**

Fig (2) Show the UV–Vis spectra of Ag-NPs prepared by ex situ irradiation process after 24hr of incubation. With the low irradiation dose, such as 1kGy and 5kGy, two peaks occurs (450, 650 nm), the peak at 450nm is the broadest and the intensity is the lowest means the nanoparticles size distribution is broadened and low yield of silver nanoparticles (Chen *et al.*, 2007). The peak at 650nm, SPR peak was shifted towards longer wavelength (Red shift), its intensity was reduced and the peak became broader, according to these changes are related to the silver particle growth (increase size) and formation of different sized particles (Puis *et al.*, 2011). With the higher irradiation dose, such as 10, 15 and 20kGy, it is a single narrow peak in the UV–Vis spectra, which means the size distribution of the silver nanoparticles is narrow. The peak intensities are higher than that in 1 and 5kGy and that means there is more yield of silver nanoparticles (Chen *et al.*, 2007). The peaks at doses 10, 15 and 20kGy are somewhat less broad than that at 1 and 5kGy; means the nanoparticles size distribution is narrow (Puis *et al.*, 2011). At a very high irradiation dose, that is 25kGy in this study, the peak is very sharp and the intensity is the highest, means there is more yield of silver nanoparticles (Chen *et al.*, 2007) than other doses, the reason can be attributed to the formation of large amount of secondary radical (organic radicals) that responsible for reduction of Ag<sup>+</sup> to Ag<sup>0</sup> by increase of irradiation dose. Time consumed to obtain maximum absorbance 24hr, since the electrochemical potential of the organic radical is more positive than that

of the Ag<sup>+</sup>/Ag<sup>0</sup> system so reaction of secondary radicals formed with Ag<sup>+</sup> ions is relatively slow (Henglein *et al.*, 1998).

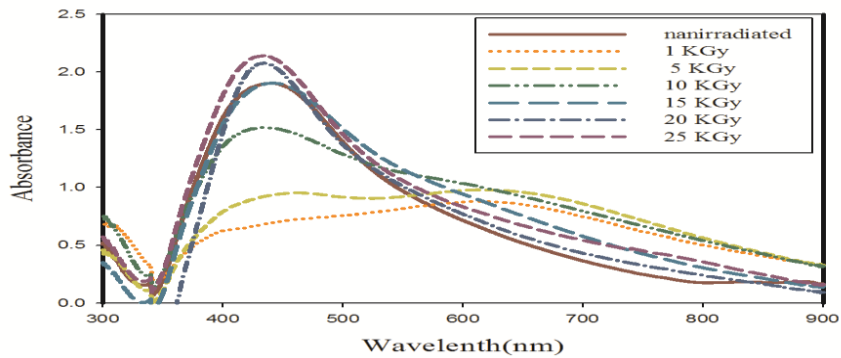


Fig (2): UV-Vis spectra of the Ag-NPs prepared by ex situ irradiation of *Monascus* supernatant.

### 3. 2. Characterization of Ag-NPs prepared by ex situ irradiation process

#### 3.2. 1. Transmission electron microscope (TEM) analysis

Control on the size, morphology and distribution of nanoparticles plays an important role in the properties of metal nanoparticles. TEM micrographs were taken into account. Fig (3a, b, c, d, e, f) Represents TEM images of Ag-NPs solution prepared by ex situ irradiation process at different doses ranged from 1 to 25kGy. Average diameter of the nanoparticles depends on dose of irradiation. The particle size distribution of the Ag-NPs prepared under irradiation (25kGy) exhibit a very narrow size distribution with average size of 7.3 nm. This result means that, the size of the prepared Ag-NPs gets smaller and the particle size distribution is improved with increasing of irradiation dose.

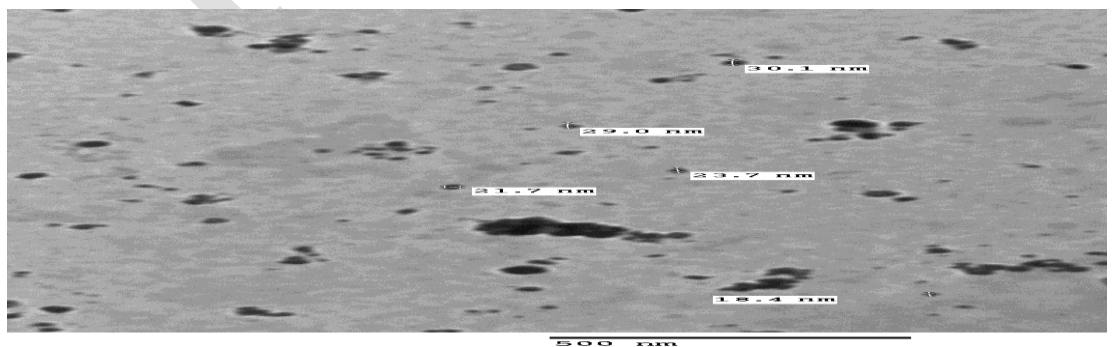
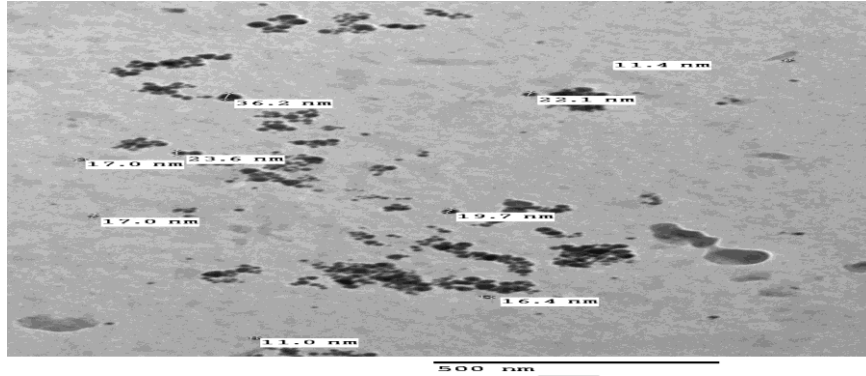
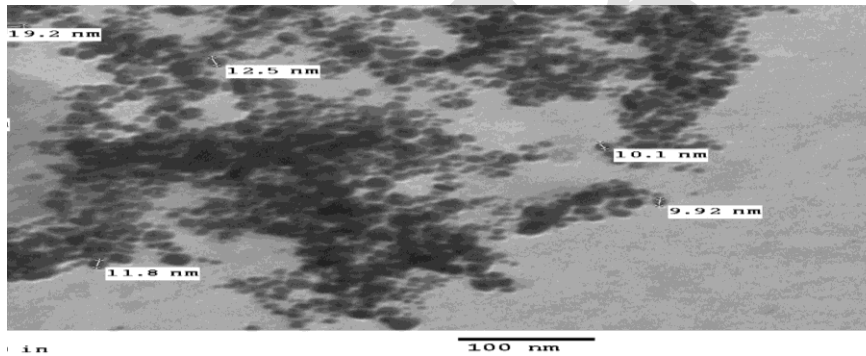


Fig (3a) 1kGyTEM micrograph of Ag-NPs prepared by ex situ irradiation *Monascus* supernatant.



**Fig (3b) 5kGyTEM micrograph of Ag-NPs prepared by ex situ irradiation *Monascus* supernatant.**



**Fig (3c) 10kGyTEM micrograph of Ag-NPs prepared by ex situ irradiation *Monascus* supernatant**

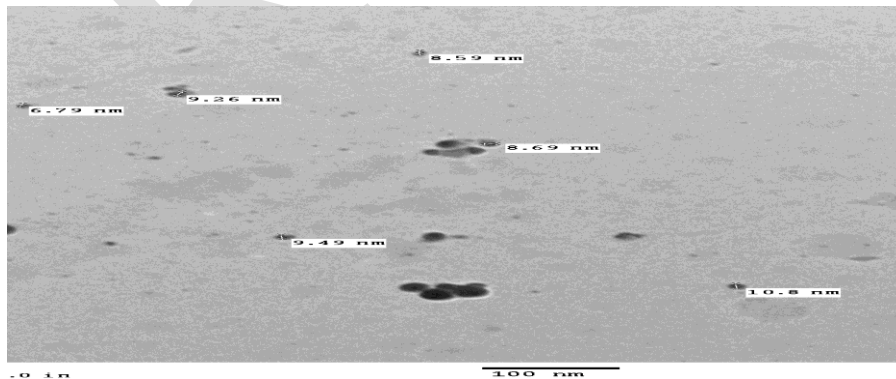


**Fig (3d) 15kGyTEM micrograph of Ag-NPs prepared by ex situ irradiation *Monascus* supernatant.**

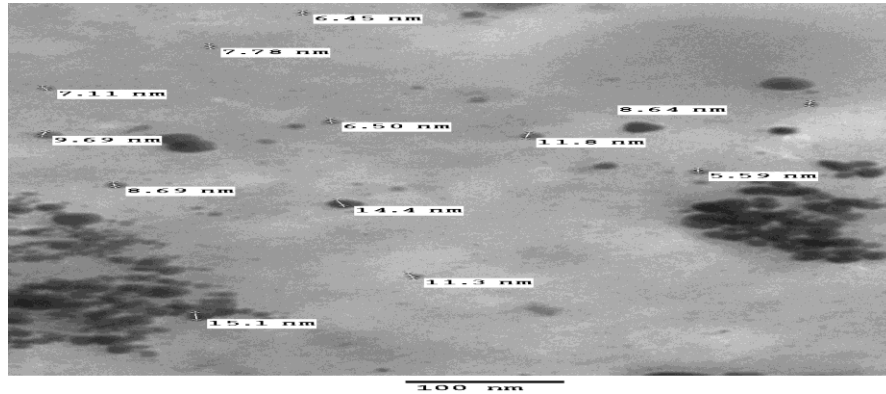


Fig (3e) 20kGyTEM micrograph of Ag-NPs prepared by ex situ irradiation *Monascus* supernatant.

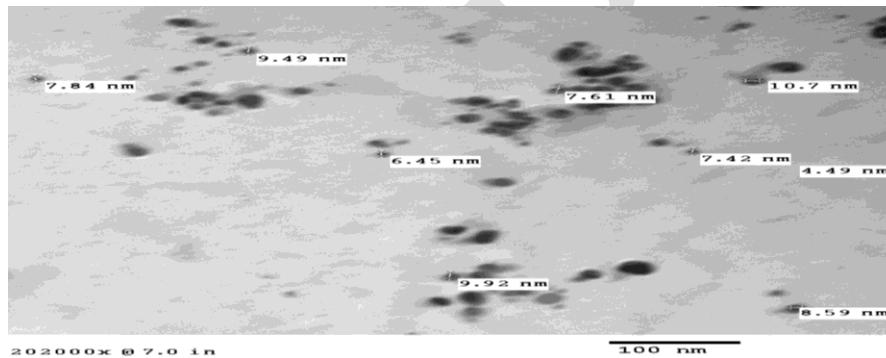
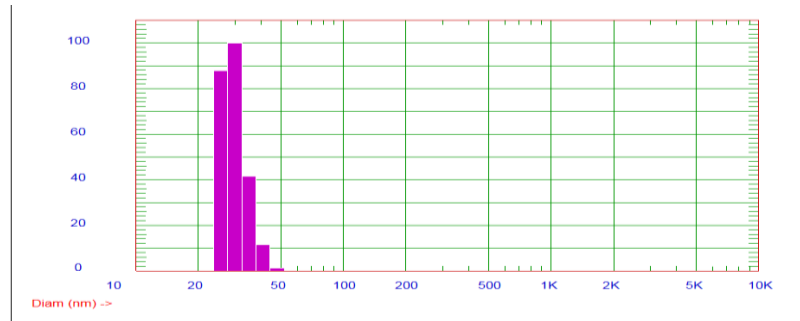


Fig (3f) 25kGyTEM micrograph of Ag-NPs prepared by ex situ irradiation *Monascus* supernatant.

### 3.2. 2. Dynamic light scattering analysis (DLS)

Average particle size was determined by DLS method and was found that the particle size and size distribution depend on dose of radiation. Fig (4a, b, c, d, e, and f) Represents DLS graphs of Ag-NPs solution prepared by ex situ irradiation process at different doses ranged from 1 to 25Kgy. Ag-NPs prepared under irradiation dose (25kGy) exhibit a very narrow size distribution with small particles size. The volume distribution of the hydrodynamic size of the nanoparticles show peak (approximately 100% of the particle volume) had its maximum size at 10.8 nm.

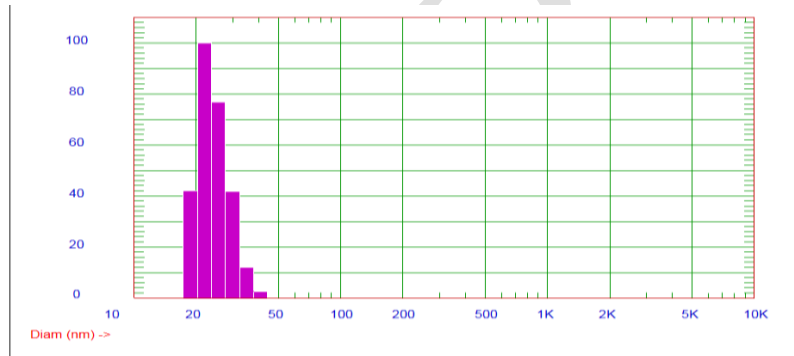
Tables (1) show Ag-NPs characters prepared under ex situ irradiation process at different doses of  $\gamma$ -irradiation.



Run\_Sample

Mean Diameter = 29.9 nm Fit Error = 6.085 Residual = 0.000

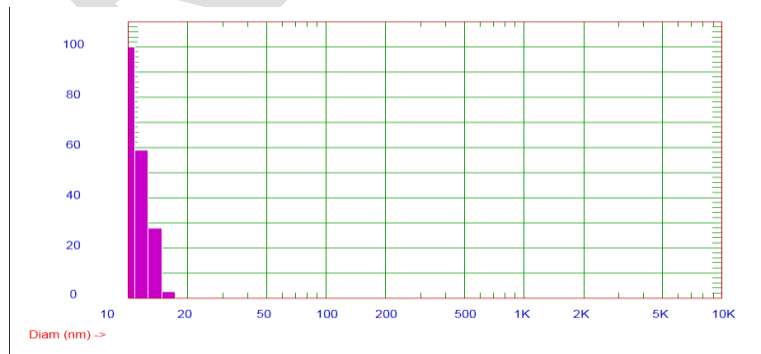
Fig (4a) 1kGy DLS graph of Ag-NPs prepared by ex situ irradiation *Monascus* supernatant



Run\_Sample

Mean Diameter = 24.6 nm Fit Error = 5.361 Residual = 19.190

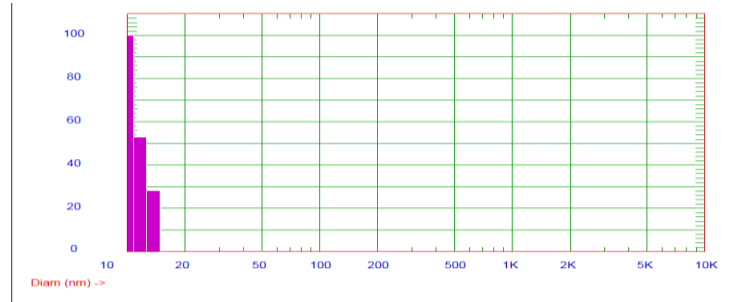
Fig (4b) 5kGy DLS graph of Ag-NPs prepared by ex situ irradiation *Monascus* supernatant.



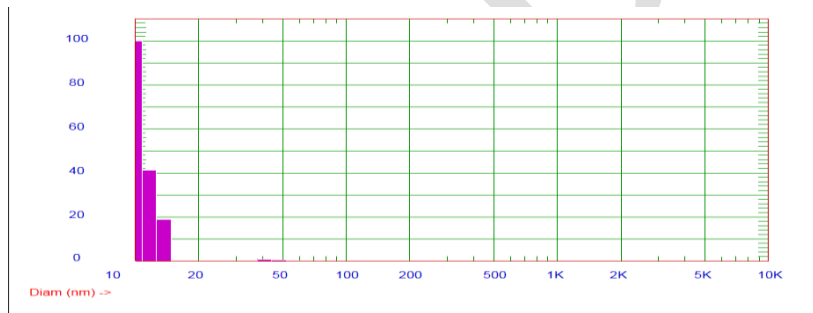
Run\_Sample

Mean Diameter = 11.2 nm Fit Error = 6.573 Residual = 11.293

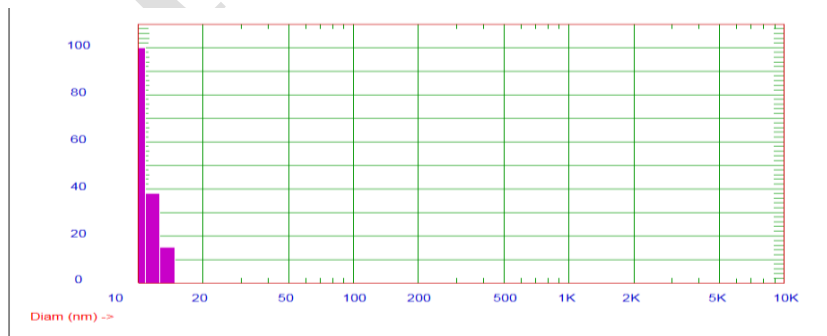
Fig (4c) 10kGy DLS graph of Ag-NPs prepared by ex situ irradiation *Monascus* supernatant.



Run\_Sample  
Mean Diameter = 11.3 nm Fit Error = 4.199 Residual = 0.000  
**Fig (4d) 15kGy DLS graph of Ag-NPs prepared by ex situ irradiation *Monascus* supernatant.**



Run\_Sample  
Mean Diameter = 11.1 nm Fit Error = 7.201 Residual = 0.000  
**Fig (4e) 20kGy DLS graph of Ag-NPs prepared by ex situ irradiation *Monascus* supernatant.**



Run\_Sample  
Mean Diameter = 10.8 nm Fit Error = 4.192 Residual = 0.000  
**Fig (4f) 25kGy DLS graph of Ag-NPs prepared by ex situ irradiation *Monascus* supernatant.**

**Table (1) Ag-NPs characters prepared under ex situ irradiation process at different doses of  $\gamma$ -irradiation.**

<b>Irradiation dose</b>	<b><math>\lambda</math> m (nm)</b>	<b>TEM average size(nm)</b>	<b>DLS average size(nm)</b>
<b>1kGy</b>	<b>420,650</b>	<b>24</b>	<b>29.9</b>
<b>5kGy</b>	<b>420,650</b>	<b>19.5</b>	<b>24.5</b>
<b>10kGy</b>	<b>420</b>	<b>12.5</b>	<b>11.3</b>
<b>15kGy</b>	<b>420</b>	<b>8.2</b>	<b>11.2</b>
<b>20kGy</b>	<b>420</b>	<b>8</b>	<b>11.1</b>
<b>25kGy</b>	<b>420</b>	<b>7.3</b>	<b>10.8</b>

### 3.2. 3. Fourier Transform Infrared Spectroscopy (FT-IR) analysis

FTIR spectra are shown in Fig (5), while the wave numbers of characteristic bands and corresponding assignments for *Monascus purpureus* supernatant and Ag-NPs thin films are listed in Table (2).

The FTIR spectrum of *Monascus purpureus* supernatant (A) exhibited the following absorption bands: broad absorption band peaking at  $3480\text{cm}^{-1}$ , corresponding to OH group vibrations, followed by a peak at  $2953\text{cm}^{-1}$ , assigned to vibration of the -CH group. Other bands in this spectrum are observed at  $1373\text{cm}^{-1}$  and  $1288\text{cm}^{-1}$ , due to the bond vibrations of the  $-\text{NO}_3$  group and of the N-OH complex, respectively. Ag-NPs spectrum (B) exhibited a few differences in peak positions compared to the *Monascus purpureus* supernatant, suggesting the bonding between *Monascus purpureus* supernatant molecules and AgNPs. One of the main differences observed is the shift of the amide carbonyl group band of *Monascus purpureus* supernatant from  $1660\text{cm}^{-1}$  toward  $1662\text{cm}^{-1}$  in the AgNPs spectrum; the shift can be attributed to the change of bond character of the N-H bond due to the nitrogen bonding with the metal. These results show that there is strong interaction in the interfaces between Ag particles and *Monascus purpureus* supernatant molecules (Davies,1988) All of the differences exhibited in the Ag-NPs spectrum (B) compared to the spectrum of *Monascus purpureus* supernatant (A) indicated the coordination bonding between nitrogen and Ag-NPs, as well as between oxygen and Ag-NPs (Jovanovic *et al.*, 2012).

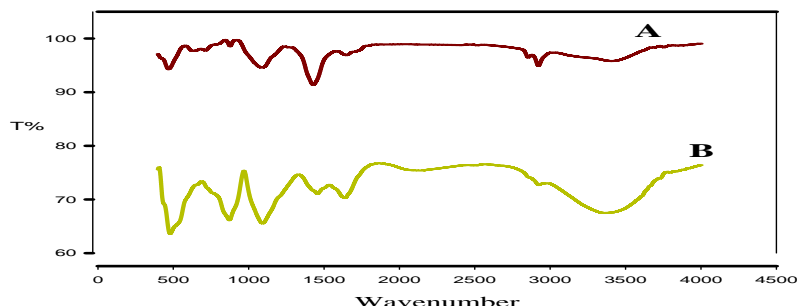


Fig (5) FT-IR spectram of *Monascus purpureus* supernatant (A) and Ag-NPs (B) prepared by ex situ irradiation process at dose 25kGy

Table (2) Wavenumber of characteristic bonds and corresponding assignments for *Monascus purpureus* supernatant and Ag-NPs under ex situ irradiation process at dose 25kG

Supernatant wavenumber	Ag-NPs wavenumber	Comment
3480	3450	OH band vibration
2953	2950	CH group vibration
1660	1662	N-C group vibration
1495	1495	Tertiary nitrogen
1373	1373	N-C=O group vibration
1288	1290	N-OH complex

### 3.3. EDX analysis of Ag-NPs synthesized by ex situ irradiation process:

Energy dispersive x-ray spectroscopy (EDX) was used to confirm that the observed granules in the solution indeed consisted of silver.

Fig (11) Show the EDX analysis revealed, the optical absorption peak was observed at approximately 3keV, which is typical for the absorption of metallic silver Nano crystallites due to surface Plasmon resonance (Kalimuthu *et al.*,2008).



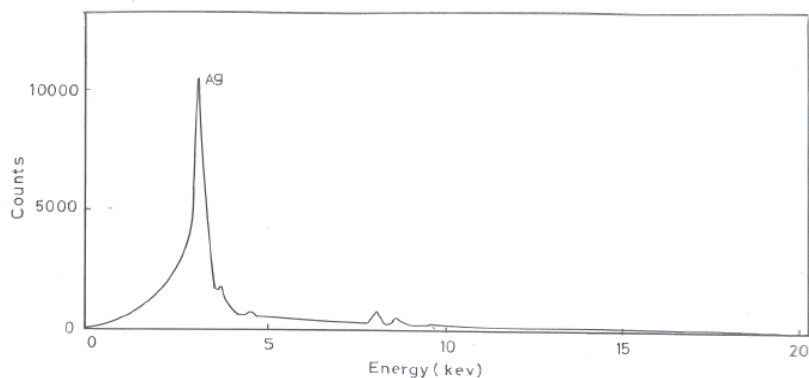


**Fig (11) EDX spectra of Ag-NPs prepared by *Monascus purpureus* supernatant under ex situ irradiation process**

### **3.4. X-ray diffraction (XRD) analysis of Ag-NPs synthesized by *Monascus purpureus* supernatant prepared by ex situ irradiation process.**

In order to verify the results of the UV–Vis spectral analysis, the sample of the Ag<sup>+</sup> ions exposed to the supernatant of the fungus was examined by XRD pattern. Fig (12) shows the XRD patterns obtained for Ag-NPs synthesized by ex situ irradiation process of fungus *Monascus purpureus* supernatant. A number of clear peaks at about 38.42°, 44.64°, 64.53°, 77.635° corresponding to the (1 1 1), (2 0 0), (2 2 0) and (3 1 1) sets of lattice planes are observed which may be indexed based on the FCC (face centered cubic) structures of silver (JCPDS file no. 03-0921). The XRD pattern thus clearly shows that the Ag-NP formed by the reduction of Ag<sup>+</sup> ions by fungus *Monascus purpureus* supernatant are crystalline in nature. The mean particle diameter of Ag-NPs was calculated from the XRD pattern according to the line width of the (1 1 1), (200), (220) and (311) planes, refraction peak using the following Scherrer equation:

$$D = K \lambda / B \cos\theta$$

Where 'λ' is wave length of X-Ray (0.1541 nm) K is a shape factor (0.9 for Ag<sup>0</sup>), 'β' is FWHM (full width at half Maximum), 'θ' is the diffraction angle and 'D' is particle diameter size. The calculated particle size details are in Table (5), mean diameter size 45nm at 25kGy.size increased in compare with TEM and DLS may be due to agglomeration of Ag-NPs and precipitation of stabilizing agents.

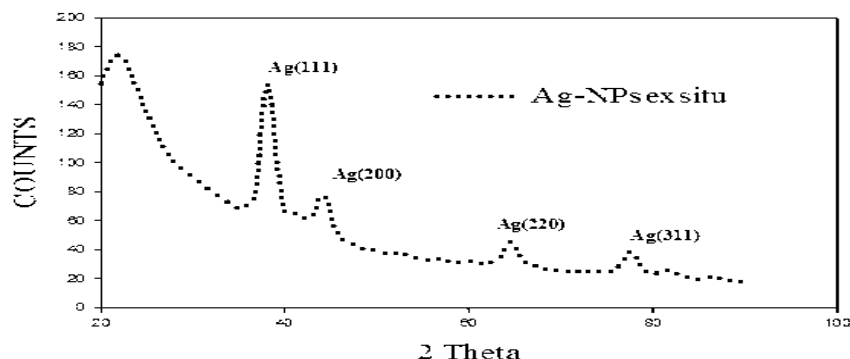


Fig (12) X-ray diffraction patterns of Ag-NPs prepared by *Monascus purpureus* supernatant under ex situ irradiation process.

Table (5) Ag-NPs size by XRD analysis prepared by ex situ irradiation at irradiation dose 25kGy

2θ of the intense peak (deg)	hKl	FWHM of Intense peak (β) radians(in situ)	Size of the particle (D) nm
38.42	(111)	0.007	21
44.64	(200)	0.003	53.6
64.53	(220)	0.004	40.8
77.635	(311)	0.003	65
Mean diameter			45

### 5. Conclusion

The preparation of silver nanoparticles was carried out by  $\gamma$ - ray irradiation under simple conditions, i.e., air atmosphere, using *Monascus purpureus* supernatant as a stabilizer. The  $\gamma$ -ray doses of 1–25kGy were sufficient to achieve maturely formed particles depend on method of irradiation process (Ex situ process). The obtained particles were spherical with size depend on radiation dose and method of irradiation; the diameter of the particles decrease with radiation dose increase, approximate size at 1kGy 24nm, at 25kGy 7.5nm. FTIR analysis has proven that the interactions in Ag NPs with *Monascus purpureus* supernatant molecules are the result of the coordination bonding between Ag NPs and nitrogen. UV–Vis spectroscopy results shown that Ag / *Monascus purpureus* supernatant investigated systems exhibited absorption band peaking at the wavelength value around 430nm confirming the presence of AgNPs.

## References

- Ahmad, M. B.; Shameli, K. and Yunus, WM.ZW.(2010) "Synthesis and characterization of silver/clay/starch bionanocomposites by green method." *Basic Appl Sci.* 4(7), 2158–2165.
- Biswal, J.; Ramnani, S. P.; Shirolkar, S. and Sabharwal, S. (2011) "Synthesis of rectangular plate like gold nanoparticles by in situ generation of seeds by combining both radiation and chemical methods." *Rad.Phys.Chem.*80, 44–49
- Carels, M. and Shepherd, D. (1977)" The effect of different nitrogen sources on pigment production and sporulation of *Monascus* sp. in submerged shaken culture." *Can J Microbiol.* 23,1360-72.
- Carvalho, J. C.; Pandey. A.; Babitha, S.and Soccol, C.R. (2003)" Production of *Monascus* biopigments an over view." *Agro Food Ind HiTec.* 14,37–42.
- Chen, Peng.; Song, Linyong .; Liu,Yankuan. and Fang,Yue. (2007)" Synthesis of silver nanoparticles by g-ray irradiation in acetic water solution containing chitosan. " *Radiation Physics and Chemistry* .76 ,1165–1168.
- Davies,M.( 1963)" *Infra-red Spectroscopy and Molecular Structure.*" An Outline of the Principles, Elsevier, Amsterdam.17.
- Eisa,Wael. H.; Abdel-Moneam,YasserK.; Shaaban,Yasser.; Abdel-Fattah, Atef . And AbouZeid AmiraM. (2011)" Gamma-irradiation assisted seeded growth of Ag nanoparticles within PVA matrix *Materials.*" *Chemistry and Physics* xxx xxx–xxx.
- Eksik, M.; Tasdelen, A.; Erciyes, Y. and Yagci, Compos. (2010)" In situ Synthesis of Oil Based Polymer/Silver Nanocomposites by Photoinduced Electron Transfer and Free Radical Polymerization Processes." *Interfaces.*17 , 357–369.
- Endo, A. (1980)" Monacolin K, a new hypocholesterolemic agent that specifically inhibits 3-hydroxy-3-methylglutaryl coenzyme A reductase." *Journal of Antibiotics.* 33, 334–336.
- Fabre, C. E.; Santerre, AL.; Loret, M. D.; Baberian,R.; Parailleux, A. and Goma. G. (1993)"Production and food application of their pigments of *Monascus* rubber." *J .Food. Sci.*58,1099–103.
- Henglein, A. (1998) "Colloidal silver nanoparticles: photochemical preparation and interaction with O<sub>2</sub>, CCl<sub>4</sub>, and some metalions." *Chem.Mater.*10,444–450.
- Janata, E. (2003) "Structure of the trimer silver cluster Ag<sub>3</sub>." *Phys. Chem* .107, 7334–7336.
- Kalimuthu, K.; Babu,R. S.;Venkataraman, D.; Bilal, M. and Gurunathan, S. (2008) " Biosynthesis of silver nanocrystals by *Bacillus licheniformis.*" *Colloids Surf. B: Bio interfaces.*65, 150–153
- Katrin, Loeschner.; Niels, Hadrup.;Klaus,Qvortrup.; Agnete, Larsen.; Xueyun, Gao.; Ulla, Vogel.; Alicja, Mortensen.; Henrik, Rye. Lam. and Erik, H. Larsen.( 2011) "Distribution of silver in rats following 28 days of repeated oral exposure to silver nanoparticles or silver acetate." Published online June 1. doi: 10.1186/1743-8977-8-18

- Kelly, K.L.; Coronado, E.; Zhao, L.L. and Schatz, G.C. (2003) "The optical properties of metal nanoparticles: the influence of size, shape and dielectric environment, *J. Phys. Chem. B* 107 668–677.
- Khanna, P.K.; Singh, N.; Charan, S.; Subbarao, V.V.S.; Gokhale, R. and Mulik, U.P. (2005) "Synthesis and characterization of Ag/PVA nanocomposite by chemical reduction method." *Mater. Chem. Phys.* 93, 117–121.
- Kim, S.S.; Rhee, S. H. and Kim, I. (1977) "Studies on production and characteristics of edible red color pigment produced by mold." *Appl Microbial Bioeng.* 11, 277–83.
- Lee, H.H.; Chou, K.S. and Huang, K.C. (2005) "Inkjet printing of nanosized silver colloids." *Nanotechnology.* 16, 2436–2441.
- Lei, Zhongli. and Fan, Youhua. (2006) "Preparation of silver nanocomposites stabilized by an amphiphilic block copolymer under ultrasonic irradiation." *Materials Letters.* 60, 2256–2260
- Li, Jun.; Kang, Bin.; Chang, Shuquan. and Dai, Yaodong. (2012) "Gamma radiation synthesis of plasmonic nanoparticles for dark field cell imaging." *Radiation Physics and Chemistry* 76, 290–1194.
- Li, W.; Seal, S. and Megan, E. (2003) "Physical and optical properties of sol gel nano-silver doped silica film on glass substrate as a function of heat treatment temperature. *J Appl Phys.* 93, 9553–9561.
- Liu, Yushenga.; Chen, Shimoua.; Lei, Zhong. and Wu, Guozhong. (2009) "Preparation of high stable silver nanoparticle dispersion by using sodium alginate as a stabilizer under gamma radiation." *Radiation Physics and Chemistry.* 78, 251–255
- Marignier, J.L.; Belloni, J.; Delcourt, M. and Chevalier, J.P. (1985) "New microaggregates of non-noble metals and alloys prepared by radiation induced reduction." *Nature.* 317, 344–345.
- Mukherjee, Gunjan. and Kumar, Singh. Sanjay. (2010) "Purification and characterization of a new red pigment from *Monascus purpureus* in submerged fermentation." *Process Biochemistry* xxx-xxx
- Murphy, C.J. (2002) "Nanocubes and nanoboxes." *Materials science* 298(5601):2139–2141.
- Naghavi, Kazem.; Saion, Elias.; Rezaee, Khadijeh. and Yunus, Wan. Mahmood. (2010) "Influence of dose on particle size of colloidal silver nanoparticles synthesized by gamma radiation." *Radiation Physics and Chemistry.* 79, 1203–1208
- Panacek, A.; Kvitek, L. and Prucek, R. (2006) "Silver colloid nanoparticles: synthesis, characterization, and their antibacterial activity. *Phys Chem.* 110, 16248–16253.
- Porel, S.; Singh, S.; S. Harsha, S.; Rao, D.N. and Radhakrishnan, T.P. (2005) "Nanoparticle-embedded polymer: in-situ synthesis, free-standing films with highly monodisperse silver nanoparticles and optical limiting." *Chem. Mater.* 17 9–12.
- Puis, J.; Adliene, D.; Guobiene, A.; Prosycevas, I. and Nalivaikoa, R. Plaipaitė. (2011) "Modification of Ag–PVP nanocomposites by gamma irradiation." *Materials Science and Engineering.* 176, 1562–1567.

- Ramnani, S.P.; Biswal, Jayashri. and Sabharwal, S. (2007) " Synthesis of silver nanoparticles supported on silica aerogel using gamma radiolysis." *Radiation Physics and Chemistry*. 76, 1290–1294.
- Rao, Y.N. ; Banerjee, D. ; Datta, A. ; Das, S.K. ; Guin, R. and Saha, A. (2010) "Gamma irradiation route to synthesis of highly redispersible natural polymer capped silver nanoparticles." *Radiation Physics and Chemistry*. 79, 1240–1246
- Remita, H.; Lampre, I.; Mostafavi, M.; Balanzat, E. and Bouffard, S. (2005) "Comparative study of metal clusters induced in aqueous solutions by  $\gamma$ -rays, electron or  $C_6^+$  ion beam irradiation. *Rad Phys Chem*. 72, 575–86.
- Shameli, K. amyari.; Ahmad, Mansor. Bin.; Yunus, Wan. Md.; Zin, Wan.; Ibrahim, Nor. Azowa. ; Gharayebi, Yadollah. and Sedaghat, Sajjad. (2010) "Synthesis of silver/montmorillonite nanocomposites using  $\gamma$ -irradiation." *International Journal of Nanomedicine*. 5, 1067–1077
- Shameli, K.; Ahmad, M.B. and Yunus, WM. ZW. (2010) "Silver/poly (lactic acid) nanocomposites: preparation, characterization, and antibacterial activity. *Int J Nanomedicine*. 5, 573–579.
- Sheikh, N.; Akhavan, A. and Kassaei, M. Z. (2009) " Synthesis of antibacterial silver nanoparticles by  $\gamma$ -irradiation. *Physica E*. 42, 132–135.
- Shimada, K.; Fujikawa, K.; Yahara, K. and Nakamura, T. (1992) "Antioxidative properties of xanthan on the antioxidation of soybean oil in cyclodextrin emulsion." *Agric. Food Chem*. 40, 945–948.
- Sun, Y. and Xia, Y. (2003) " Gold and silver nanoparticles: a class of chromophores with colors tunable in the range from 400 to 700 nm." *Analyst*. 128, 686–691.
- Temgire, M. K. and Joshi, S. S. (2004) " Optical and structural studies of silver nanoparticles." *Radiation Physics and Chemistry*. 71, 1039–1044.
- Tripathy, M.; Ashok, Chrs.; karam, N. C. Prathna. and Mkherrjee. Amitaya. (2010) " Process variables in biomimetic synthesis of silver nanoparticles by aqueous extract of *Azadirachta indica* (Neem) leaves. " *Nanopart Res*. 12, 237–246
- Yang, Qing. ; Wang, Feng. ; Tang, Kaibin. ; Wang, Chunrui. ; Chen, Zhiwen. and Qian, Yitai. (2002) " The formation of fractal Ag nanocrystallites via  $\gamma$ -irradiation route in isopropyl alcohol Materials." *Chemistry and Physics*. 78, 495–500.
- Zagoldie, Pandey. Sonil.; Shah, Ritu. and Sharon, Madhuri. (2012) " Extracellular Fabrication of Silver Nanoparticles using *Pseudomonas aeruginosa* and its Antimicrobial Assay." *Advances in Applied Science Research*. 3 (3), 1776-1778.
- Zhao, G. R.; Xiang, ZJ. ; Ye, T.X. and Guo. Z.X. (2006) "antioxidant activities of *salvia miltiorrhiza* and *panax notoginseng*." *food chemistry*. 99, (4). 767